Division of Symbiotic Systems

Professor
KAWAGUCHI, Masayoshi

Associate Professor
SOYANO, Takashi

Assistant Professor:	*TAKEDA, Naoya*
Technical Staff:	*FUKADA-TANAKA, Sachiko*
Visiting Scientist	*NAKAGAWA, Tomomi*
Postdoctoral Fellow:	*FUJITA, Hironori*
	KOBAYASHI, Yuuki
	NAGAE, Miwa
	MAEDA, Taro
	KAMEOKA, Hiromu
	SHIMIZU-MITAO, Yasushi
	TOKUMOTO, Yuji
	OKUMA, Nao
SOKENDAI Graduate Student:	*TSUZUKI, Shusaku*
	NISHIDA, Hanna
	FUKUHARA, Mai
	LIU, Meng
Technical Assistant:	*SUZAKI, Momoyo*
	OGAWA, Yuko
	YOSHINORI, Yumi
	TOKAIRIN, Asami
	ODA, Akiko
Secretary:	*OKUBO, Masayo*

Rhizobium–legume symbiosis is one of the most successful mutually beneficial interactions on earth. In this symbiosis, soil bacteria called rhizobia supply the host legumes with ammonia produced through bacterial nitrogen fixation. In return, host plants provide the rhizobia with their photosynthetic products. To accomplish this biotic interaction, leguminous plants develop nodules on their roots. On the other hand, more than 80% of land plant families have symbiotic relationships with arbuscular mycorrhizal (AM) fungi. Despite marked differences between the fungal and bacterial symbioses, common genes are required for both interactions. Using a model legume *Lotus japonicus*, we are trying to unveil the molecular mechanisms of both symbiotic systems.

I. Root nodule symbiosis

1-1 A third CLE peptide systemically controls nodulation in *L. japonicus*.

In root nodule symbiosis, a mutual relationship between leguminous plants and nitrogen-fixing rhizobia, the mechanism for the autoregulation of nodulation (AON) plays a key role in preventing the production of an excess number of nodules. AON is based on long-distance cell-to-cell communication between roots and shoots. Among the 39 *CLAVATA3/ESR-related* (*CLE*) peptide genes identified from *Lotus japonicus*, the expression of *CLE-ROOT SIGNAL 1* (*CLE-RS1*) and *-RS2* is induced immediately in response to rhizobial inoculation after direct activation by an RWP-RK type transcription factor NODULE INCEPTION (NIN). CLE-RS1 and -RS2 peptides act as putative root-derived signals that transmit signals inhibiting further nodule development through interaction with a shoot-acting receptor-like kinase HYPERNODULATION ABERRANT ROOT FORMATION 1 (HAR1). A loss-of function mutation in the *HAR1* gene significantly increases nodule numbers. Hence, the CLE-RS1/2–HAR1 pathway is hypothesized to play a pivotal role in the negative regulation of nodulation in AON. KLAVIER (KLV), another shoot-acting LRR-RLK, seems to be involved in CLE-RS1/2-mediated negative regulation of nodulation. Recently cytokinin production was reported to be induced in the shoot by the downstream part of the CLE-RS1/2–HAR1 signaling pathway. In addition, shoot-applied cytokinin is able to move to roots and inhibit nodulation. These results suggest that shoot-derived cytokinin may be a shoot-derived inhibitor (SDI) candidate. There might be a proteasome-mediated degradation process for an unidentified protein in the most downstream part of AON in roots because the negative effect of shoot-applied cytokinin is masked by a mutation in the F-box protein TOO MUCH LOVE (TML). Although our knowledge of AON has been furthered, identification of additional components of AON will be undoubtedly essential for a deeper understanding of the mechanism.

In order to identify new *LjCLE* genes, we referred to a new database that has a reference sequence data set containing the *L. japonicus* genome assembly Lj2.5 and the unique de novo assembled contigs derived from *L. japonicus*. A BLAST search using the amino acid sequence of a CLE domain from CLE-RS1 as a query enabled us to identify five new CLE peptides. Among the CLE peptides identified, *CLE-RS3* and *LjCLE40* expression was induced in inoculated roots. A hairy root transformation study showed that constitutive expression of *CLE-RS3* in the roots significantly reduced nodule number not only in transformed but also in untransformed roots. On the other hand, the CLR-RS3-mediated suppression of nodulation activity was masked in the *har1* and *tml* plants. These results suggest that CLE-RS3 is a new component of AON in *L. japonicus* that may act as a potential root-derived signal.

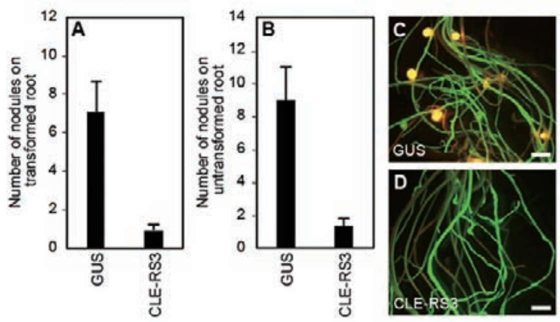

Figure 1. Number of nodules formed on transformed (A) and untransformed (B) roots of the wild-type plants that have transgenic hairy roots constitutively expressing *GUS* or *CLE-RS3* (n = 14–20 plants). The nodulation phenotype of the plants that have transgenic hairy roots constitutively expressing *GUS* (C) or *CLE-RS3* (D) at 21 days after inoculation. Transgenic roots were identified by GFP fluorescence. The *Mesorhizobium loti* strain that constitutively expresses *DsRED* was used in these experiments. Error bars indicate SE. Scale bars 2 mm.

1-2 Thiamine biosynthesis is required for nodule development.

Thiamine (vitamin B1) is an essential nutrient to produce energy. Thiamine is synthesized through a multiple-step pathway and functions in the form of a thiamine pyrophosphate. Thiamine is assembled from pyrimidine and thiazole moieties. In *L. japonicus*, THI1 and THI2 (a THI1 paralog) catalyze the biosynthesis of the thiazole moiety, and THIC catalyzes the biosynthesis of the pyrimidine moiety.

The phenotypes of thiamine-deficient mutants of *L. japonicus* are summarized in Figure 2. *THIC* is expressed in all tissues and is a single copy gene in *L. japonicus*. The *thiC* mutant showed chlorosis in the leaves (Figure 2A), which is a typical and lethal phenotype observed in the thiamine-deficient plants. *THIC* expression was induced in nodules, and the nodule number also showed a reduction in the *thiC* mutant. However, it is not clear that the nodulation defect in the *thiC* mutant is caused by the loss of *THIC* function, because the chlorosis resulted in severe growth defects which also caused a decrease of nodule formation. Therefore, we also analyzed *THI1* function in nodulation. *THI1* is highly expressed in roots, nodules, and seeds, whereas *THI2* is expressed mainly in shoots. The *thi1* mutant did not have chlorosis in the leaves and showed no significant growth defects, although the knockdown plants of *THI2* gene displayed chlorosis and growth defects. The *thi1* mutant showed reduced nodule and seed size (Figure 2B, C), and the phenotypes were suppressed by exogenous thiamine treatment. The analyses indicated that thiamine affects the early stage of nodule development. These results demonstrated that THI1 is involved in both nodule development in roots and seed maturation in shoots, excluding the effects of chlorosis and growth defects.

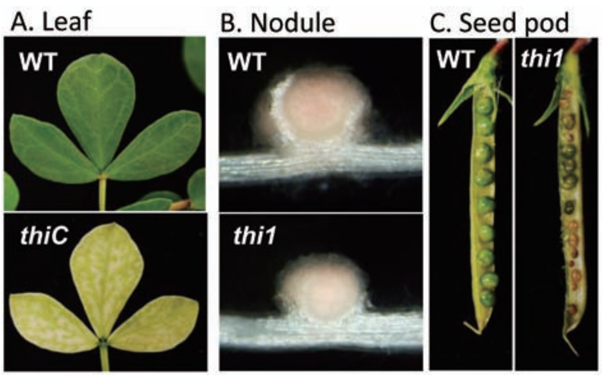

Figure 2. Thiamine-deficient phenotypes in *thiC* and *thi1* mutants of *L. japonicus*. The *thiC* mutant showed chlorosis in leaves (A). The nodule size decreased in the *thi1* mutant (B). The *thi1* mutant also showed abnormal phenotypes in seed formation (C).

On the other hand, we could not observe obvious AM colonization phenotypes in the *thi1* mutant or thiamine-treated plants. However, it has been reported that the AM fungus *Rhizophagus irregularis* lacks thiamine biosynthesis genes. Thiamine is essential for living organisms, therefore, AM fungus should require a thiamine supply from the host plant. We think that further analysis is required to reveal thiamine function and effect on AM in both the host plant and AM fungus.

II. Improvement of referential AM fungus genome

Arbuscular mycorrhiza (AM) is a mutualistic plant-fungus interaction that confers great advantages to growth and survival on the land. However, the molecular biological mechanisms governing the symbiotic relationships remain largely unknown. The fragmented genome data of AM fungi (AMF) had been one of the barriers for the molecular biological study of AM. Although the genome of a model strain of AMF, *R. irregularis* DAOM-181602, has been sequenced in multiple studies, these genomic data were made up of over 28,000 short sequences (N50 = 4-16kbp). Thus, previous data was difficult to use for comparative genomics with other fungal species.

To facilitate the molecular biology of AMF, we improved *R. irregularis* whole-genome data using PacBio-based *de novo* sequencing. As a result, the total size of our 210 contigs reached 97.2 % (149.75 Mbp) of the predicted genome size (154 Mb), and its N50 length elongated to 2.2 Mbp. Compared to previous analyses, the genome completeness in total assembly size increased 6-39 points, the number of assemblies decreased by135-144 fold, and N50 length became about 140-551 times longer (Figure 3). This improvement of the statistics validated the availability of the PacBio sequencing to the repeat-rich genome.

From the new assemblies, we constructed 37,711 protein-coding genes. This gene model comprised 94% of the fungal core conservative genes, suggesting high genetic completeness of our gene model set. However, our genomic data did not contain some of the key genes for the typically present metabolic pathway in autotrophic fungi (e.g., Thiamine synthesis). This is credible evidence of gene loss in *R. irregularis* genomes, and supports the previous opinion that AMF are unable to produce those essential nutrients. AMF may obtain the nutrients from the host plant. Overall, we succeed in providing a high-quality reference genome data for the molecular understanding of AM.

III. Pattern density control in self-organized pattern formation

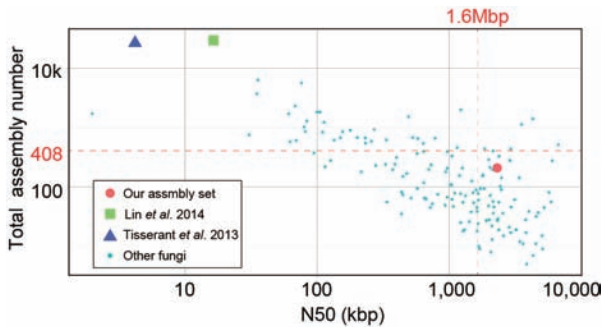

Figure 3. Assembly statistics of *R. irregularis* and other fungus genomic data. The correspondence between the symbols and the assembly sets are presented in the boxed legend. The statistics (total assembly size and N50 length) from *R. irregularis* were presented with larger symbols. The other 153 fungal genomes from the RefSeq database are presented with blue dots. The horizontal and vertical red lines represent averages of total assembly numbers and N50 length of the 153 fungal genomes.

Many self-organized patterns have been explained by the concept of the Turing mechanism, in which interactions between diffusible molecules initiate spatial instability to translate into stable patterns. Whether or not spatial instability is induced can be determined by conventional linear stability analysis. In contrast, resulting spatial patterns produced by such instability depend on nonlinear effects of the model dynamics and are difficult to be predicted without numerical simulations.

In two-dimensional space, patterns generated by the Turing system are divided into three types: spot patterns, stripe patterns, and reverse spot patterns (Figure 4, upper panels). It is reported that these pattern types are associated with the relative position of the equilibrium between lower and upper constraints in the activator–inhibitor system, one of the best-known Turing systems. That is, spot, stripe, and reverse spot patterns are formed when the equilibrium is closer to the lower limit, around the middle of the two limits, and closer to upper limit, respectively.

We here report that pattern density, proportion of area with high concentrations of the activator molecule, is strongly correlated with R_{eq}, the relative position of the equilibrium between the upper and lower constraints, in linear dynamics of the activator–inhibitor system (Figure 4). Furthermore, we demonstrate that this finding can be successfully applied to the well-known phenomenon of animal skin color pattern formation and to the patterning of stomatal lineage. This relationship between equilibrium position and pattern density is also observed in various nonlinear dynamics. Accordingly, this finding could be widely applicable to self-organized patterns and would be a powerful and reliable tool for elucidating the underlying mechanism of self-organized pattern formations in biological systems.

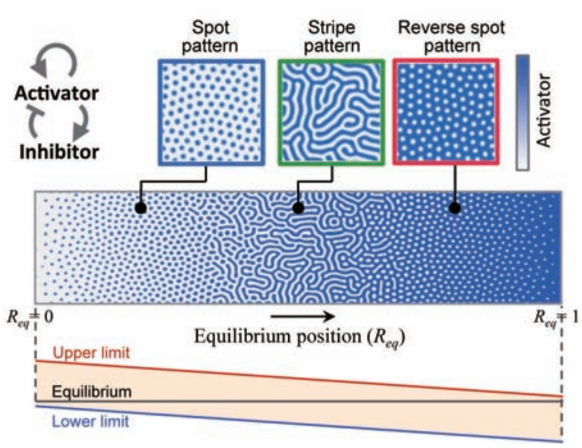

Figure 4. Pattern density control by activator-inhibitor dynamics with upper and lower constraints in two-dimensional space. Pattern density (proportion of area with high activator concentrations) increases as equilibrium becomes apart from lower limit and close to upper limit (i.e. R_{eq} increases). Insets show activator distributions that correspond to spot pattern (R_{eq} = 0.2), tripe pattern (R_{eq} = 0.5), and reverse spot pattern (R_{eq} = 0.8).

Publication List:

〔Original papers〕

- Kameoka, H., Dun, E.A., Lopez-Obando, M., Brewer P.B., de Saint Germain, A., Rameau, C., Beveridge, C.A., and Kyozuka, J. (2016). Phloem transport of the receptor DWARF14 protein is required for full function of strigolactones. Plant Physiol. *172*, 1844–1852.
- Kikuchi, Y., Hijikata, N., Ohtomo, R., Handa, Y., Kawaguchi, M., Saito, K., Masuta, C., and Ezawa, T. (2016). Aquaporin-mediated long-distance polyphosphate translocation directed towards the host in arbuscular mycorrhizal symbiosis: application of virus induced gene silencing. New Phytol. *211*, 1202-1208.
- Malolepszy, A., Mun, T., Sandal, N., Gupta, V., Dubin, M., Urbański, D., Shah, N., Bachmann, A., Fukai, E., Hirakawa, H., Tabata, S., Nadzieja, M., Markmann, K., Su, J., Umehara, Y., Soyano, T., Miyahara, A., Satoh, S., Hayashi, M., Stougaard, J., and Andersen, S. (2016). The LORE1 insertion mutant resource. Plant J. *88*, 306-317.
- Miyata, K., Hayafune, M., Kobae, Y., Kaku, H., Nishizawa, Y., Masuda, Y., Shibuya, N., and Nakagawa, T. (2016). Evaluation of the role of the LysM receptor-like kinase, OsNFR5/OsRLK2 for AM symbiosis in rice. Plant Cell Physiol. *57*, 2283-2290.
- Miyata, K., and Nakagawa, T. (2016). The *Lotus* intrinsic ethylene receptor regulates both symbiotic and non-symbiotic responses. Plant Biotech. *33*, 27-32.
- Nagae, M., Parniske, M., Kawaguchi, M., and Takeda, N. (2016). The thiamine biosynthesis gene *THI1* promotes nodule growth and seed maturation. Plant Physiol. *172*, 2033-2043.
- Nagae, M., Parniske, M., Kawaguchi, M., and Takeda, N. (2016). The relationship between thiamine and two symbioses: root nodule symbiosis and arbuscular mycorrhiza. Plant Signal. Behav. *11*, e1265723.
- Nishida, H., Handa, Y., Tanaka, S., Suzaki, T., and Kawaguchi, M. (2016). Expression of the CLE-RS3 gene suppresses root nodulation in *Lotus japonicus*. J. Plant Res. *129*, 909-919.
- Sakurai, K., Tomiyama, K., Kawakami, Y., Ochiai, N., Yabe, S., Nakagawa, T., and Asakawa, Y. (2016). Volatile components emitted from the liverwort *Marchantia paleacea* subsp. *diptera*. Nat. Prod. Commun. *11*, 263-264.
- Tokumoto, Y., and Nakagawa, M. (2016). Climate-induced abortion and predation: reproductive success of the pioneer shrub *Dillenia suffruticosa* in Malaysian Borneo. J. Trop. Ecol. *32*, 50-62.
- Tokumoto, Y., Kajiura, H., Takeno, S., Harada, Y., Suzuki, N., Hosaka, T., Gyokusen, K., and Nakazawa, Y. (2016). Induction of tetraploid hardy rubber tree, *Eucommia ulmoides*, and phenotypic differences from diploid. Plant Biotechnol. *33*, 51-57.
- Tsuzuki, S., Handa, Y., Takeda, N., and Kawaguchi, M. (2016). Strigolactone-induced putative secreted protein 1 is required for theestablishment of symbiosis by the arbuscular mycorrhizal fungus Rhizophagusirregulars. Mol. Plant Microbe Interact. *29*, 277-286.

〔Original paper (E-publication ahead of print)〕

- Yano, K., Aoki, S., Liu, M., Umehara, Y., Suganuma, N., Iwasaki, W., Sato, S., Soyano, T., Kouchi, H., and Kawaguchi, M. Function and evolution of a *Lotus japonicus* AP2/ERF family transcription factor that is required for development of infection threads. DNA Res. 2016 Dec 27.